Front. Earth Sci. 2016, 10(3): 432–443
DOI 10.1007/s11707-015-0535-2

RESEARCH ARTICLE

A one-way coupled atmospheric-hydrological modeling system with combination of high-resolution and ensemble precipitation forecasting

Zhiyong WU[1], Juan WU (✉)[1,2], Guihua LU[1]

1 College of Hydrology and Water Resources, Hohai University, Nanjing 210098, China
2 Bureau of Hydrology Information Center of Taihu Basin Authority, Shanghai 200434, China

Abstract Coupled hydrological and atmospheric modeling is an effective tool for providing advanced flood forecasting. However, the uncertainties in precipitation forecasts are still considerable. To address uncertainties, a one-way coupled atmospheric-hydrological modeling system, with a combination of high-resolution and ensemble precipitation forecasting, has been developed. It consists of three high-resolution single models and four sets of ensemble forecasts from the THORPEX Interactive Grande Global Ensemble database. The former provides higher forecasting accuracy, while the latter provides the range of forecasts. The combined precipitation forecasting was then implemented to drive the Chinese National Flood Forecasting System in the 2007 and 2008 Huai River flood hindcast analysis. The encouraging results demonstrated that the system can clearly give a set of forecasting hydrographs for a flood event and has a promising relative stability in discharge peaks and timing for warning purposes. It not only gives a deterministic prediction, but also generates probability forecasts. Even though the signal was not persistent until four days before the peak discharge was observed in the 2007 flood event, the visualization based on threshold exceedance provided clear and concise essential warning information at an early stage. Forecasters could better prepare for the possibility of a flood at an early stage, and then issue an actual warning if the signal strengthened. This process may provide decision support for civil protection authorities. In future studies, different weather forecasts will be assigned various weight coefficients to represent the covariance of predictors and the extremes of distributions.

Keywords one-way coupled hydrological and atmospheric modeling, flood forecast, high-resolution precipitation forecasting, ensemble prediction

Received October 1, 2014; accepted May 31, 2015

E-mail: wujuan3412@163.com

1 Introduction

Floods are among the most commonly occurring natural disasters in China. The increased development and population in the floodplains has intensified the vulnerability for such disasters in these flood-prone areas (Rossa et al., 2011). Consequently, an increase in flood damage is foreseeable in the country, even if climate change is not taken into account. The Huai River Basin (HRB), located in eastern China, is one such flood-prone area, consisting of south-north climate transition bands (Zhang et al., 2011). For centuries, complex and changeable climate conditions, abundant precipitation, numerous floodgates, and intense human activity led to disastrous upstream and downstream floods (Liu et al., 2013), on the Wangjiaba cross section.

High-resolution mesoscale numerical weather prediction (NWP) models have remarkably enhanced the accuracy and lead time of precipitation forecasting over the past few decades (Liu et al., 2009; Pappenberger et al., 2011; Pan et al., 2012; Li and zou, 2014). The accurate and timely flood forecasts can be demonstrated by the coupling of hydrological models with precipitation forecasting of NWP models, known as coupled hydrological and atmospheric modeling (CHAM). The CHAM method is particularly important for mountainous regions, where flood forecasting depends on the rapid availability of precipitation forecasts. Diomede et al. (2008a) coupled the non-hydrostatic meteorological Lokal Model with the distributed rainfall–runoff TOPKAPI model to complete discharge forecasting over the Reno River Basin. The coupling of these two models demonstrated that the high-

resolution meteorological model configuration can considerably improve the forecast for both total amount and timing of rainfall.

Even though the scale compatibility between atmospheric and hydrological models no longer represents a serious problem for the CHAM method, single-model precipitation forecasts often lack quality and are unreliable for driving hydrological models. Considerable uncertainty in precipitation forecasts (Diomede et al., 2008b) still exists at scales of interest for hydrological purposes. Aimed at evaluating precipitation uncertainties, Davolio et al. (2012) focused on comparing two different multi-analysis ensemble approaches on the short-to-medium range in a recent severe weather episode that affected the Reno River Basin. Quantifying uncertainties in flood forecasting is a difficult task that involves multiple nonlinear model components in the system (Pappenberger et al., 2013). A few studies have suggested that probabilistic forecasts are necessary due to the numerous and varied outcomes that can influence the decision-making process (Krzysztofowicz, 2001; Liguori and Ramirez, 2013). However, many forecasters prefer deterministic forecasts (Todini, 2004), which may prevent the appropriate use of probabilistic forecasts and increase the number of false alarms. Therefore, the principal research goal should focus on improving precipitation forecasts at mesoscale spatial and temporal scales. One approach is the combination of a high-resolution and an ensemble modeling system. Some studies have found that lower-resolution model ensemble forecasts provide greater accuracy than higher-resolution model forecasts (Stensrud et al., 1999). Implementing both approaches is useful in the hydrological forecasting process (Roebber et al., 2004). Davolio et al. (2008) proposed a meteo-hydrological forecasting system to implement real-time configuration for several episodes of intense precipitation that affected the Reno River Basin, demonstrating the high potential for the coupled system to predict discharge peaks for warning purposes, while the ensemble hydrological forecasts provide a range of possible flood scenarios for the decision support of civil protection authorities.

In this paper, a one-way coupled atmospheric-hydrological modeling system, with a combination of high-resolution and ensemble precipitation forecasting, is presented. The system consists of three high-resolution, single-model forecasts and four sets of ensemble forecasts from The Observing System Research and Predictability Experiment (THORPEX) Interactive Grand Global Ensemble database, collectively known as the TIGGE database (Froude, 2010). The high-resolution forecasts provide higher forecasting accuracy, while the ensemble forecasts provide a range of forecasts. Thus, the system not only gives a deterministic prediction, but also gives probability forecasts. The combination of high-resolution with ensemble precipitation forecasting was implemented in 2007 to drive the Chinese National Flood Forecasting System (NFFS) in the 2007 Huai River flood hindcast analysis.

2 The coupled atmospheric-hydrological modeling system

The system consists of three high-resolution single models and four sets of ensemble forecasts from the TIGGE database. The former provides higher forecasting accuracy, and the latter provides the range of forecasts. The system schemes of our study are shown in Fig. 1.

2.1 Chinese National Flood Forecasting System (NFFS)

The NFFS, developed by the Bureau of Hydrology (BOH) and affiliated with the Ministry of Water Resources (MWR), is used to generate flood forecasts (Zhang, 2006). As a robust, full-functional, and user-friendly system, the NFFS is capable of providing timely and accurate flood forecasts. First, based on the standard structure of the forecasting database, the NFFS develops various standard forecasting models and absorbs already available forecasting methods to form a model base, which enable users to find and manage forecasting schemes flexibly by selecting a set of models and methods. Second, the NFFS uses the functions of both interactive and automatic timing forecasting to ensure timeliness and ease. Third, by using the observed precipitation and future weather conditions provided by NWP, the NFFS permits flood forecasting for different lead-times and accuracy requirements in local hydrologic centers and key reservoirs, with flood control and detention basins. The first function provides data correction and simulated results information, which includes precipitation input, model parameters, rating curve, and adjustment optimization by graphical interface. The second function allows the NFFS to automatically accomplish flood forecasts based on forecasting scheme.

2.2 High-resolution precipitation forecasting models

The high-resolution inputs of the NFFS consist of three models: the Canadian regional Mesoscale Compressible Community Model (MC2), the Global Environmental Multiscale (GEM) model, and the T213L31 global spectral model (T213).

The MC2 is a three-dimensional, limited-area, high-resolution NWP model developed at the Meteorological Services of Canada (MSC), which employs fully elastic, non-hydrostatic equations and the semi-implicit, semi-Lagrangian algorithm (Tanguay et al., 1990). The MC2, with the Interactions Soil-Biosphere-Atmosphere (ISBA) land surface scheme (Noilhan and Planton, 1989; Habets et al., 1999), is configured on a Mercator projection with 409 $\times$ 301 $\times$ 40 grid points. Details of MC2 dynamics and

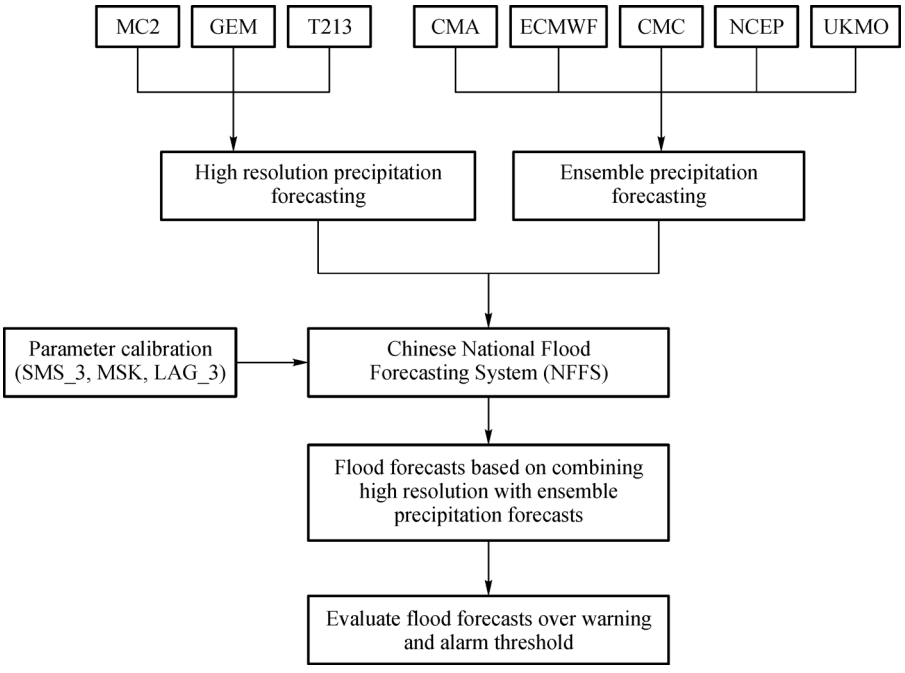

Fig. 1 Coupled atmospheric-hydrological modeling system flood forecast schemes flowchart.

physics were discussed in Benoit et al. (1997) and Wen et al. (2000). The Canadian Meteorological Centre (CMC) global 1-km topographic data set is used for setting up the MC2. The ISBA parameters are initialized using CMC global archived land-surface and atmospheric data sets. The MC2 is initialized and driven at the boundaries by using the CMC operational 96-hour forecasts of the GEM model (Côté et al., 1998). Various studies have shown that the MC2 is accurate and efficient over a wide spectrum of scales, ranging from micro-scale supersonic waves, through small-scale convection, to large-scale synoptic weather systems (Laprise et al., 1997; Benoit et al., 2001). We ran the MC2 at a horizontal resolution of 20 km up to 96 hours in advance over the Wangjiaba Basin in this study.

The GEM model was developed by the Meteorological Research Branch (MRB) in partnership with the CMC. The GEM model was originally developed as a unique dynamical core that would be versatile enough to replace both the hemispheric model, formerly used in Canada for regional short-range forecasting, and the global spectral model, used for medium-range forecasting (see Côté et al., 1998). The GEM model achieved this versatility by using a variable-resolution horizontal mesh that allows a concentration of the grid points over an area of interest. The GEM model became the operational model for regional forecasting in 1997 and for medium-range forecasting in 1998. The operational GEM model dynamics are formulated in terms of the hydrostatic primitive equations with a terrain-following vertical pressure coordinate. The time discretization is an implicit two-time-level semi-Lagrangian scheme. The spatial discretization is a Galerkin grid-point formulation on an Arakawa C-grid in the horizontal and an unstaggered vertical discretization. Starting in 2003, the non-hydrostatic dynamics of the GEM model were adapted to run on a limited-area domain, using lateral boundary specifications from Thomas et al. (1998) for the semi-Lagrangian transport and the elliptic solver. The latter is an adaptation of the global solver described in Qaddouri et al. (2000). The lateral boundary conditions are those developed by Yakimiv and Robert (1986). A growing number of meteorological and environmental applications are now either based on or use the GEM model (Erfani et al., 2003). In this study, we ran the GEM model over the Wangjiaba Basin at a horizontal resolution of 33 km up to 96 hours in advance.

The National Meteorology Center (NMC) of China has utilized the T213 as the operational numerical model since 2002 (Ma et al., 2007). As a global spectral model, the T213 has a maximum truncated wave number of 213 waves in the horizontal over approximately 60 km and 31 layers of vertical mixed coordinates. The model adopts a semi-Lagrangian temporal integration scheme. It contains a set of advanced physical processes, including radiation scheme, parameterized sub-grid point terrain drag, and parameterized convection of mass flux, turbulence diffusion, clouds, large-scale precipitation, and soil and surface processes. The T213 model has more advanced physical parameterizations and its own data assimilation system (optimal interpolation). Over a period of time, many researchers have focused on forecast accuracy and discussed specific synoptic parameters of the T213

model after operational use, particularly for precipitation. The results indicate improvement in the T213 model's forecast accuracy over the previous version. In the present study, we ran the T213 model over the Wangjiaba Basin at a horizontal resolution of 60 km up to 96 hours in advance.

2.3 Ensemble precipitation forecasting system

The ensemble forecasts inputs of the NFFS are based on TIGGE data. TIGGE is a World Weather Research Program project. The TIGGE network aims at providing a collaboration platform to improve the development of ensemble weather predictions around the world (Bao et al., 2011). The TIGGE network now covers vast regions across the globe with adequate detail for flood forecasting (Pappenberger et al., 2008) and will likely become a heavily used archive. The 0-240 h precipitation forecasts of four ensemble prediction systems, or EPSs, (CMA, ECMWF, NCEP, and UKMO) were obtained from the TIGGE-ECMWF archiving center located over the Wangjiaba sub-basin. Each center provides one "central" unperturbed analysis generated by a data-assimilation procedure and a number of forecasts with perturbed initial conditions (He et al., 2009). All forecast members were assigned equal weights (Park et al., 2008) in this study. Table 1 shows the main properties of the four EPSs evaluated in this study. For the initial-condition perturbations, the CMA uses the bred vectors approach (BVs), the CMC uses the ensemble Kalman filter approach (EnKF), the ECMWF uses the singular vectors approach (SVs; Buizza and Palmer, 1995; Bourke et al., 2004), the UKMO uses an ensemble-transform Kalman filter (ETKF) approach (Bishop et al., 2001), and the NCEP uses an ensemble-transform (ET) method (Wei and Toth, 2003). The ECMWF applies random perturbations to the parameterized physical processes (stochastic physics) and the UKMO uses the Shutts kinetic energy backscatter algorithm. Other main characteristics of the different EPSs, such as the number of ensemble members and resolutions, are listed in Table 1.

In our study, four flood-forecasting schemes are established in the Wangjiaba Basin, including the Xixian, Bantai, and Huangchuan sub-basins, and also in the intermediate region from the three sub-basins to the outlet. The three-sources saturation excess model (Zhao, 1992) is applied in runoff yield forecasting, the Muskingum routing method (Gill, 1978) is applied in computing channel routing generation, and the lag-and-route method (Luo and Qian, 1987) is applied in the configuration of watershed flow concentration forecasting. On the basis of these model applications, the present study favors six-hour precipitation as inputs of the NFFS. Before the current study, we calibrated the parameters of the coupled atmospheric-hydrological model with historical rainfall-runoff data for the Wangjiaba Basin, with a calibration period from January 1991 to December 2005. The calibration was done by using rain gauge precipitation and hydrographs at the Wangjiaba cross section. First, we applied a Thiessen polygon to delineate coverage by the 49 rain gauges and the model grid points. Second, we used the sub-basin digital elevation model information to determine the runoff that drains into the upper sub-basin. The Wangjiaba outlet hydrograph can thus be decomposed into four major components: outflows from Xixian, Huangchuan, and Bantai and runoff generated by the intermediate region from the three sub-basins to the Wangjiaba outlet. Third, we applied the runoff generation module via the three-source saturation excess model (SMS_3). We then used the Muskingum routing method (MSK) to compute channel routing generation. Last, we summed the outflow from each sub-basin to obtain the Wangjibaba outlet hydrograph by the lag-and-route method (LAG_3). The calibrated model parameters were not changed during the forecasting in this study.

3 Meteorological and hydrological features of case study

Focused on the severe flood event triggered by prolonged heavy torrential precipitation that occurred in the HRB from July 5 to July 10, 2007, we analyzed the hindcast of the Wangjiaba cross section, where heavy precipitation rapidly collects upstream and transitions to low-lying flood plains. The Wangjiaba Basin, a sub-basin of the HRB with an area of 30,500 km^2, plays a vital role in flood control and management for the entire region and is thus of great interest to the Office of State Flood Control and Drought Relief Headquarters of China. Hence, the Huai River Basin Commission of the Ministry of Water Resources expended numerous resources to provide more accurate and timely flood forecasts over the Wangjiaba cross section, ranked as

Table 1 Meteorological forecast centers used in this study (Froude, 2010)

Center	Horizontal resolution	No. of levels	No. of members	Initial perturbation	Perturbation model physics
CMA	0.5625°×0.5625°	31	14	BVs (globe)	No
CMC	1.2°×1.2°	28	20	EnKF (globe)	Yes
ECMWF	0.45°×0.45°	62	50	SVs (globe)	Yes
UKMO	1.25°×0.83°	38	23	ETKF (globe)	Yes
NCEP	0.9474°×0.9474°	28	20	ET (globe)	No

the highest priority and most difficult for operational flood management decision making (Zhao et al., 2012; Ma et al., 2014; Yu et al., 2014). The rain gauges, hydrological stations, and sluices used in this sub-basin are presented in Fig. 2.

The region received two to three times more precipitation from July 5 to July 10, 2007 than typically experienced over the HRB during the same time period, leading to the second largest flood since 1954, with more than 20 million people affected and a 12-billion CNY loss. The intensive precipitation of 2007 in a typical Meiyu season (Si et al., 2009) could be ascribed to the stability of the western Pacific subtropical high (WPSH) and a strong lower-level jet stream. With a shear line providing a favorable condition for the development of convection, the ridge line of the WPSH remained quasi-stationary between 25°N and 27°N, leading to an extensive interaction between the southern warm humid air and the northern cold air over the HRB (Xuan et al., 2009).

The 24-hour observed rainfall accumulation amounts were divided into six categories: light rain = 0.1 to 9.9 mm, moderate rain = 10 to 24.9 mm, heavy rain = 25 to 49.9 mm, rainstorm = 50 to 99.9 mm, heavy rainstorm = 100 to 199.9 mm, and torrential rain = more than 200 mm. Three distinct periods of rainfall can be classified based on observed precipitation. The first period, from 8:00 July 5 to 8:00 July 6, occurred over the northern sections of the Wangjiaba sub-basin. The northward advance of the WPSH was responsible for the increasing wind speed in southern China, which was a main factor in the formation of the lower-level jet stream until July 5. Intense precipitation affected the entire basin during the second period, from July 6 to July 7. This area can be considered as a fingerprint of the Lake Baikal trough and vortex, with a shear line moving eastward. Maximum amounts of rainfall (< 50 mm) occurred within the 24-hour period of 8:00 on July 8 to 8:00 on July 9, mainly over the southern part of the basin (Fig. 3(d)). Precipitation ceased to affect the Wangjiaba sub-basin during the third period, from July 9 to July 10. These lower levels of precipitation were attributed to the northward move of the WPSH, while the shear line moved to the south of the Yangtze River. The water stage of the Wangjiaba cross section was 29.46 m at 12:00 midnight on July 10, exceeding the alarm stage (29.30 m). At 12:28 a.m., the brake was taken off the Wangjiaba sluice to release water into the Mengwa flood detention area. The maximum discharge was 8,100 m^3/s at 20:00 on July 10, including the mainstream, Shangang, Wangjiaba sluice, and Dilicheng. The observed daily precipitation (mm) during the period from July 5 to July 10 is shown in Fig. 3(a) to Fig. 3(f).

4 Results analysis and discussion

4.1 Forecasts of high-resolution models

The meteorological model runs started at 20:00, July 5, 2007. The 96-hour forecasts were divided into four consecutive 24-hour accumulated precipitation amounts, and the four forecast ranges, corresponding to 0–24, 24–48, 48–72, and 72–96 hours, were named the first phase, second phase, third phase, and fourth phase, respectively. When analyzing the accuracy of 24-hour and 96-hour accumulated precipitation amounts, we adopted two principles to define acceptable results. The first principle states that for a given 24-hour period, a forecast is deemed acceptable if the relative percentage error of the accumulated amount is within ±50% of the gauge observations. The second principle states that if the 24-hour accumulated amount at a gauge is less than 5 mm, and the corresponding forecast is less than 10 mm, the forecast is also considered successful. A forecast success rate is achieved by dividing the number of forecasts by the number of acceptable results.

Figure 4 presents observed and forecasted precipitation averaged over the Wangjiaba Basin during the July 5–8, 2007 event, when all forecast dates had acceptable results,

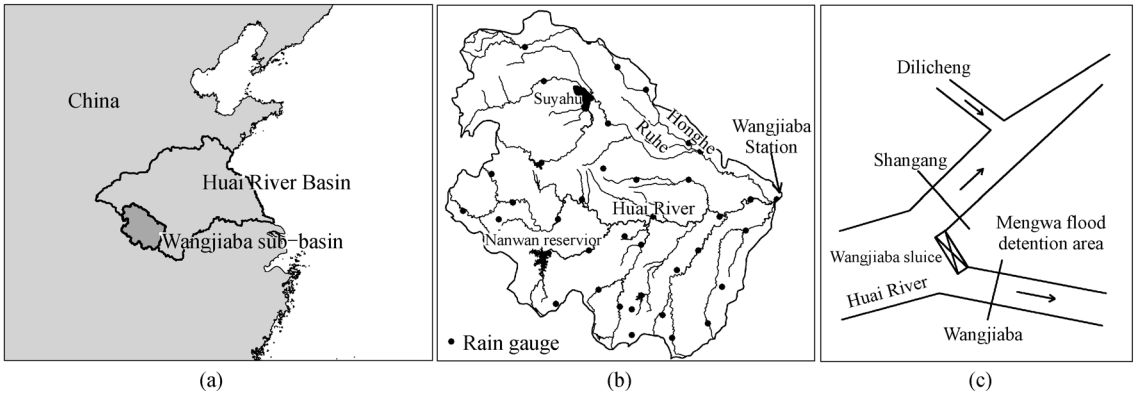

Fig. 2 (a) Wangjiaba sub-basin and Huai River Basin in China, (b) rain gauges and hydrological stations in Wangjiaba sub-basin, and (c) schematic diagram of the location of Wangjiaba sluice, Shangang, Dilicheng, and Wangjiaba.

except on July 6. As compared with the observed maximum 24-hour precipitation values greater than 70 mm, the GEM model and the T213 model underestimated precipitation amounts in the fourth phase of July 5 and third phase of July 6. The MC2 provides a good estimate in the fourth phase of July 5, with a relative percentage error of 9%, which ascribed that high-resolution models had better performances for evaluating the sensitivity of different initial conditions (Davolio et al., 2008). However, with an unsatisfactory degree of accuracy, the MC2 underestimated the precipitation amount for the second phase, but overestimated the amount for the third phase of July 7. The advantages of the T213 model are demonstrated in the second phase of July 7 and the first phase of July 8, with relative percentage errors of 10% and 3%, respectively. The MC2, and the GEM and T213 models forecast success rates for the 24-hour accumulated precipitation amounts are, 62.5%, 50%, and 56.25%, respectively. In most situations, the MC2 model precipitation forecasts outperformed those of the GEM and T213 models throughout the whole period.

The discharge forecast of the NFFS was completed at 6 hour intervals, and the observed precipitation was updated hourly. The response of the NFFS, forced by the different precipitation forecasts, is shown in Fig. 5. The MC2 model of July 5, run at a higher resolution, showed greater accuracy than the GEM and T213 models in the discharge forecast, both in time evolution and in peak. The MC2, and also the GEM and T213 models, significantly underestimated the observed peak discharge on July 6 due to severe precipitation estimation, especially for the third forecast phase of July 6. The MC2 lagging peak discharge of July 7 weakened the advantages of high-resolution models, which can be attributed to underestimating the main precipitation peak for the second phase, but overestimating the precipitation for the third phase. Alternatively, the GEM and T213 models filled the instability gap of the MC2 with proper discharge peak and time. Errors in the MC2 and the GEM and T213 model forecasts are corrected by the up-to-date observed precipitation. Therefore, the accuracy of daily flood forecasts can be improved accordingly.

4.2 Combining high resolution with ensemble forecasts based on the TIGGE database

Under more "predictable" regimes, users would expect the differences between successive forecasts to be small, with a greater spread expected under more "volatile" regimes. However, it may be difficult for an ensemble to provide an improved forecast under more "predictable" conditions, because individual deterministic forecasts would be expected to do quite well on their own (Dalcher et al., 1988). If an ensemble forecast were to perform significantly better, this improvement would constitute a strong robust test (Branković et al., 1990). As has been shown in previous sections, the ranges of high-resolution forecasts were not always stable, despite the better resolution of the weather phenomenon on some forecast dates. A conclusion drawn about the phenomenon from the rolling forecasting

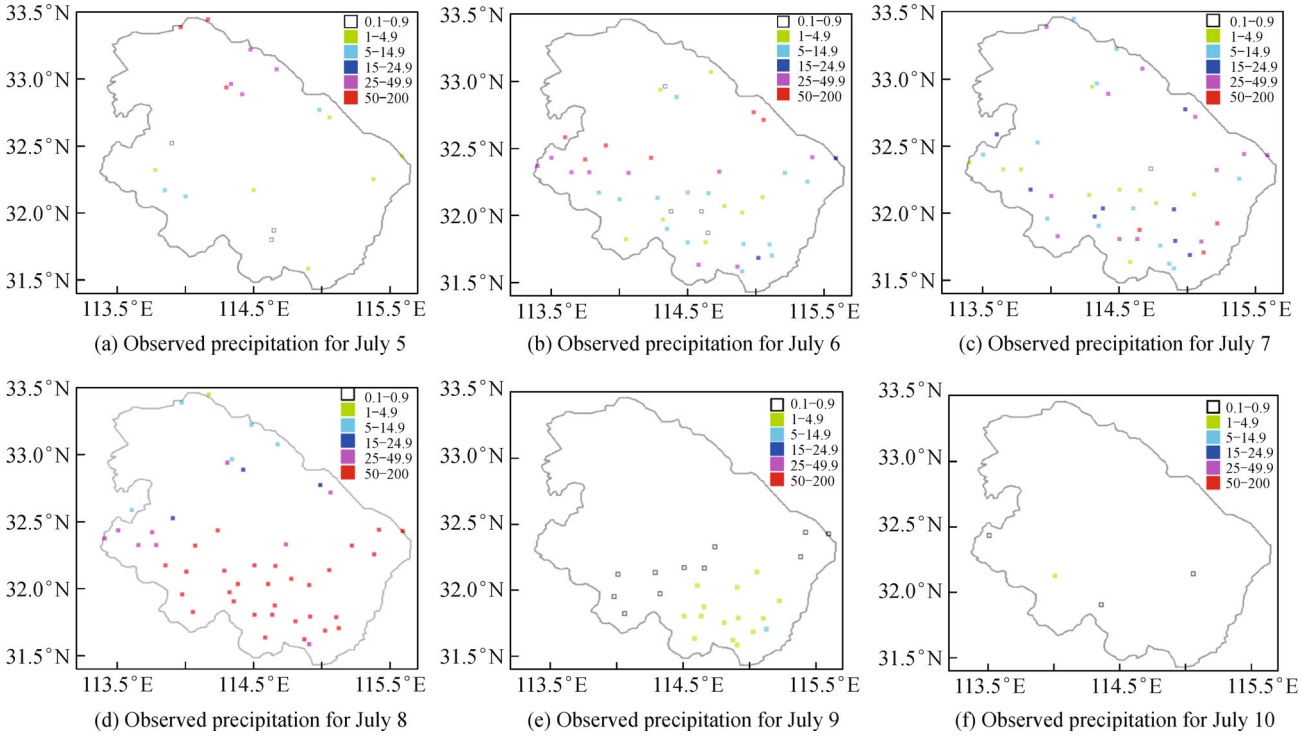

Fig. 3 Observed daily precipitation (mm) during the period from July 5 (a) to July 10 (f) in 2007, averaged over the Wangjiaba Basin.

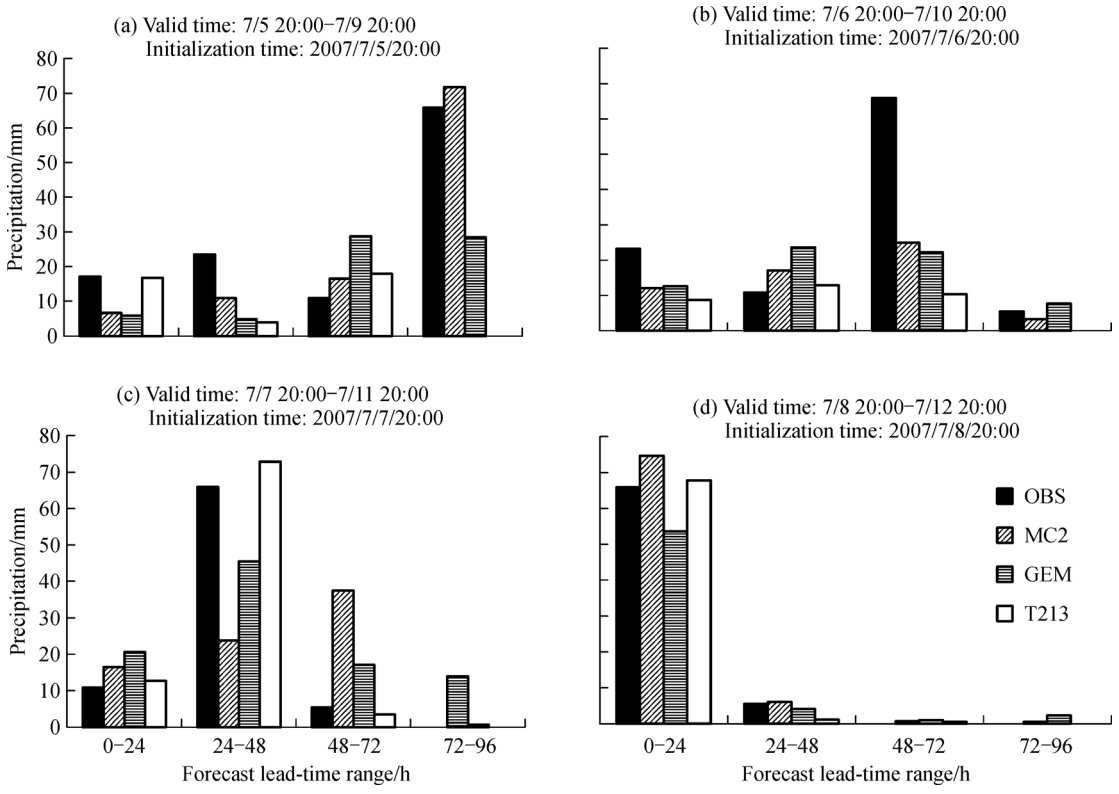

Fig. 4 Observed and forecast precipitation for the 96-hour period initialized from 20:00 July 5 (a) to July 8 (d) in 2007, averaged over the Wangjiaba Basin.

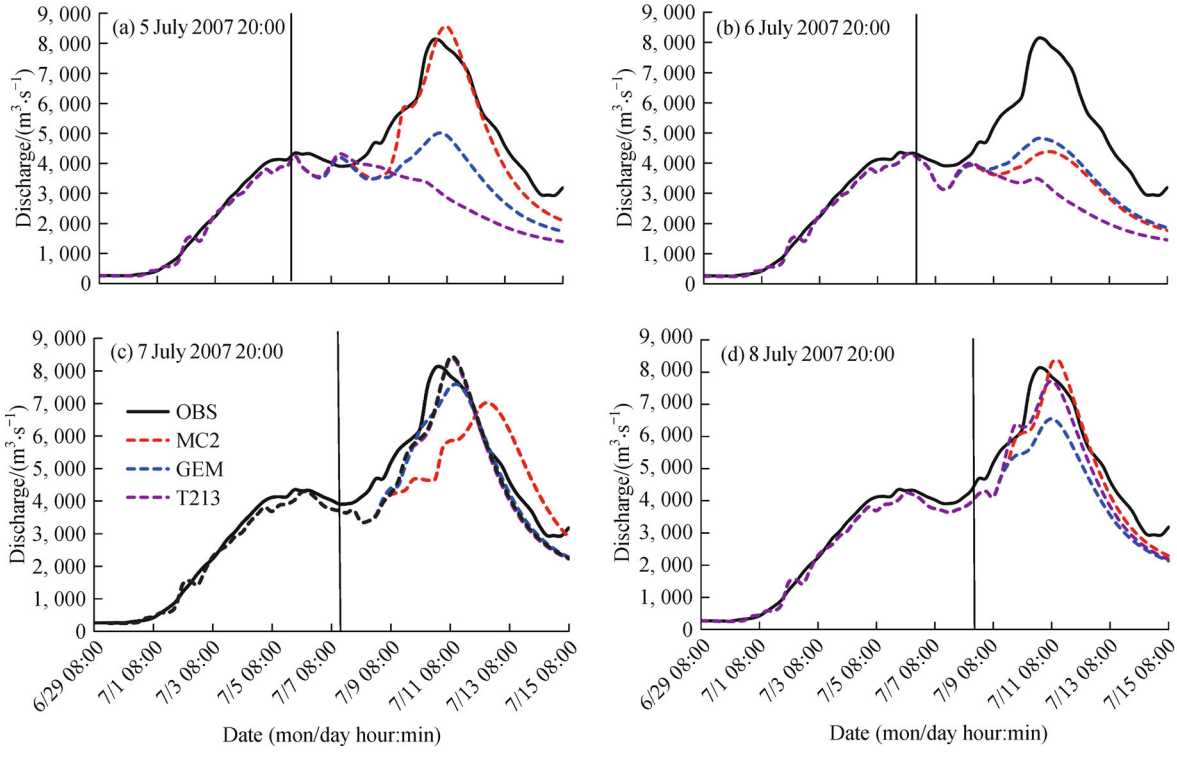

Fig. 5 Flood forecast of high resolution models and observed hydrographs at the Wangjiaba Station from July 5 (a) to July 8 (d), 2007. The long, dashed vertical lines indicate the starting time of each forecast. The observed hydrograph is shown in black, and the colored dashed hydrograph uses the MC2 and the GEM and T213 models forecasts.

system was that the accuracy was not always inversely proportional to the forecast ranges or lead times. In other words, forecasts with longer lead times may have higher precision than those with shorter lead times. Based on the fact that the ensemble forecasts may also be more accurate than individual forecasts, we used all forecasts with different resolutions to compose a grand ensemble (GE), not only of the forecast date, but also of the previous dates, to provide guidance on the most likely scenario, which may be useful for flood forecasting. The ensemble forecasts are composed of seven members in the present study. The TIGGE EPS for each center was averaged, and then put through the hydrological model, which leads to four ensemble mean predictions from the four selected centers. These four are then put together with the earlier reported three high-resolution forecasts to make a seven-member GE forecast for the first day. The lagging starts on the second day, making a 14-member ensemble, a 21-member ensemble, and a 28-member ensemble.

With the initial data for each member of the ensemble lagged by 24 hours, discharge forecasts can be created for 6-hour windows, corresponding to the range of 6-hourly intervals: 2:00, 8:00, 14:00, and 20:00. The 28 forecasts are used to produce a discharge forecast that is equally weighted, which provides a sample of statistics and thus can be used to construct probabilistic forecasts. Figure 6 features the discharge forecast in the July 5–8, 2007 event. The GE consisted of all seven members on each day. All the forecasts of GE issued on July 5, 2007 were distributed separately, with the MC2 displaying the best agreement for the observed discharge hydrograph. The peak discharges of other forecasts were much lower than the observed forecast. It was supposed that the MC2 with high resolution (20 km) had a good performance in predicting peak discharge and peak time. However, the discharge forecasts of July 6 and 7 demonstrated that the conventional rules were not always applicable, due to the very poor performance of the MC2 peak discharge on July 6 and peak time on July 7. With the passage of forecasting dates, the forecast members demonstrated a fairly consistent signal, representing an intensive flood event. On the other hand, the exact peak time fluctuated between July 10 and July 12, while the peak discharge ranged from 4,300 to 8,600 m^3/s due to the scattered spread of different models. However, the progress of agreement among forecasts from long to short lead times showed that the forecasts become more predictable closer to the actual event. The situation improved on July 8, 2007 when most forecast members clustered closer to each other than on the previous forecasting dates (nearly 60% members agreed on the observed peak).

A decision-making element needed to be incorporated into a flood forecast to determine whether or not the discharge would exceed a critical threshold. In the operational practice, a flood event at the Wangjiaba cross section was defined when the water level reached or passed the value of 27.5 m above the waste Yellow River Datum level, corresponding to a discharge value of 2,820 m^3/s.

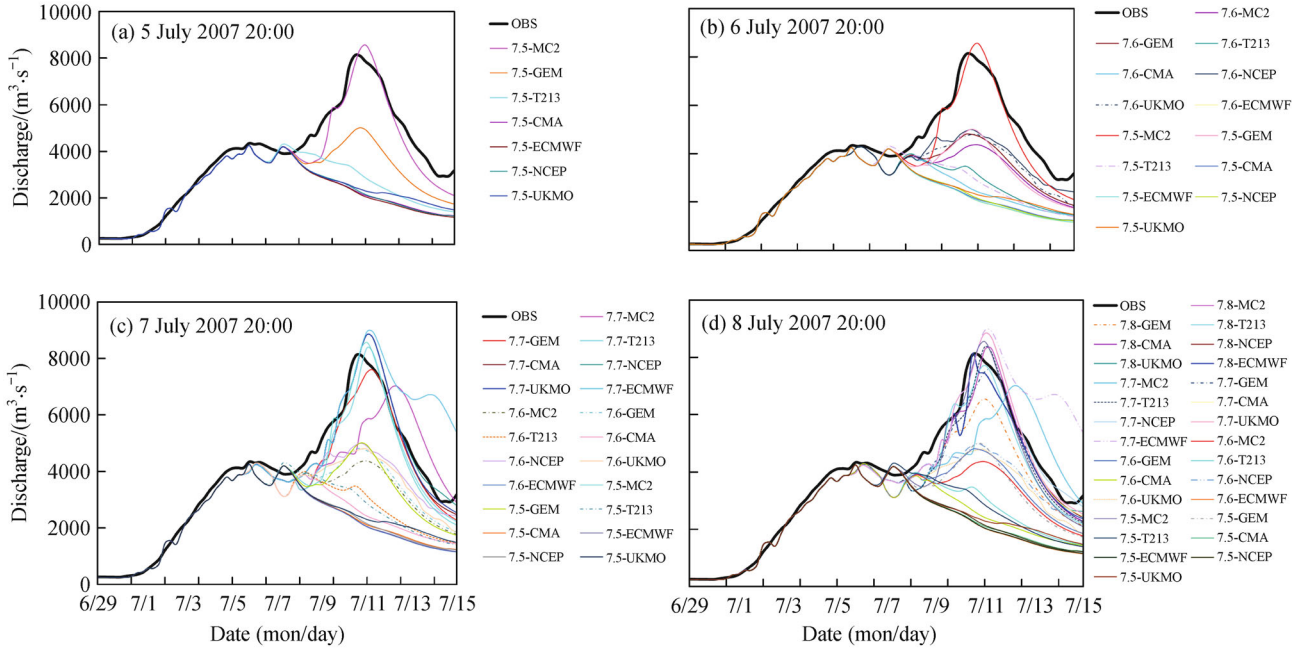

Fig. 6 Combination of high resolution flood forecasts with ensemble forecasts and observed hydrographs at the Wangjiaba Station from July 5 (a) to July 8 (d), 2007. The long dashed vertical lines indicate the starting time of each forecast. The observed hydrograph is shown in black, and the model forecasts are shown in color.

This value represents the warning threshold, while the alarm level is set to 29.3 m above the waste Yellow River Datum level, corresponding to a discharge value of approximately 5,579 m^3/s. In this study, the forecasting discharge was ranked from highest to lowest, with the two values stated above chosen as critical thresholds. The discharge time series are then transformed into different exceedances by taking into account the two critical thresholds for forecasting discharges associated with different quantiles. Figure 7 features the percentages above the warning and alarm threshold for the studied event, demonstrating increasing potential for detection at an early stage. The visualization based on threshold exceedance provided essential, clear and concise, early warning information, with 66% above the warning threshold and 28% above the alarm threshold. However, the signal was not persistent until four days before the peak discharge was observed. Even though the percentages were not expressed exactly in the simplified colored box, the visualization of forecast persistence, which could be the real warning if the signal exceeds a certain percentage, is represented.

4.3 Discussion

The system efficiency is composed of meteorological model precision and hydrological model accuracy. In this study, we used a combined high-resolution, single-forecast and ensemble prediction mode, which makes the rainfall forecast uncertainties an objective description. The hydrological model parameters were calibrated based on historical flood data, which ensures the stability of the model. These parameters provide a certain level of efficiency for the future application of the coupling model. The encouraging results of the 2007 case study demonstrated that combining high resolution with ensemble forecasts based on the TIGGE database provided a promising relative stability in discharge peaks and timing for warning purposes. To further verify the system, we also give the results of a 2008 case showing the capability of the model to effectively predict 2008 floods. Figure 8 shows that most forecast members were more closely clustered, with 62.5% of members agreeing on the observed peak on August 15, 2008, when the forecast members demonstrated a consistent intensive flood signal. The spread of the different models was not scattered, and the exact peak time fluctuated between August 18 and August 19, reaching to more than 50% probability (Fig. 9).

The advantage of using multi-source precipitation forecasts was to gain long lead time, which provided more information at an earlier stage and potentially increased the ability to detect a flood episode. The flood was visible in some centers at the early age, although the probability is low. The signal was not persistent until 4 days before the peak discharge was observed in 2007 flood study. The Forecasters could better prepare for the possibility of a flood at an early stage, and then issue the real warning if the signal strengthens. In addition, warning threshold and the alarm level were determined from long-term observed river discharge instead of simulated

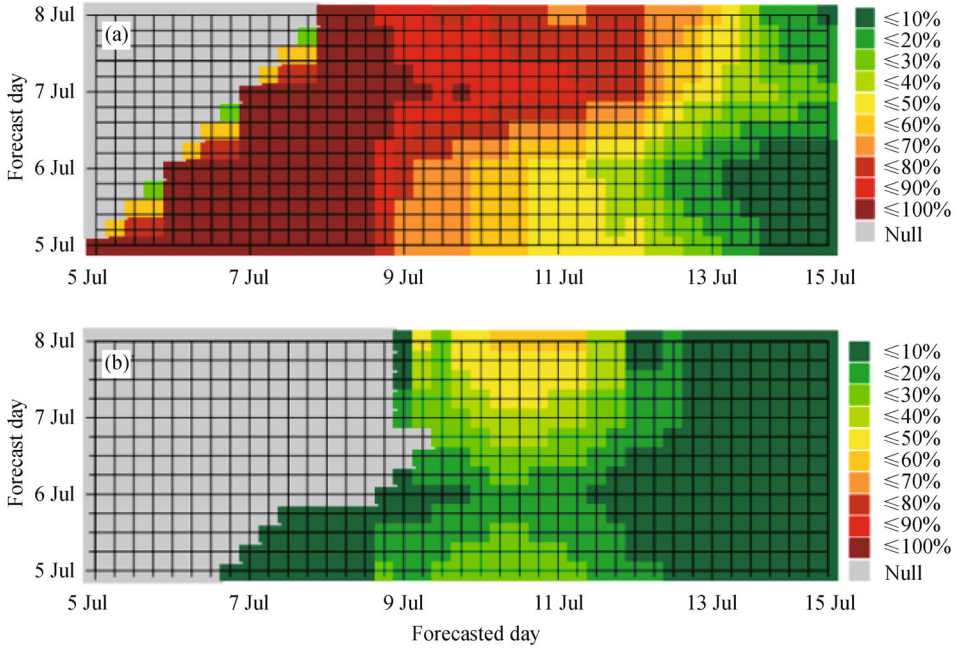

Fig. 7 Percentages above the warning (a) and alarm (b) thresholds for the 2007 flood event. The vertical axis represents the starting time of GE forecast, and the abscissa is the lead time.

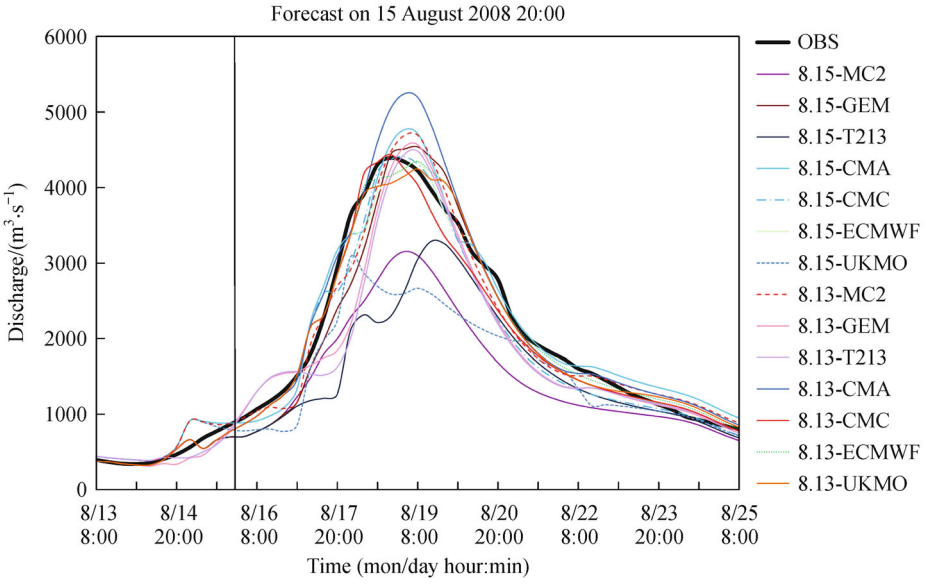

Fig. 8 The observed and forecasted hydrographs at the Wangjiaba Station on August 15, 2008.

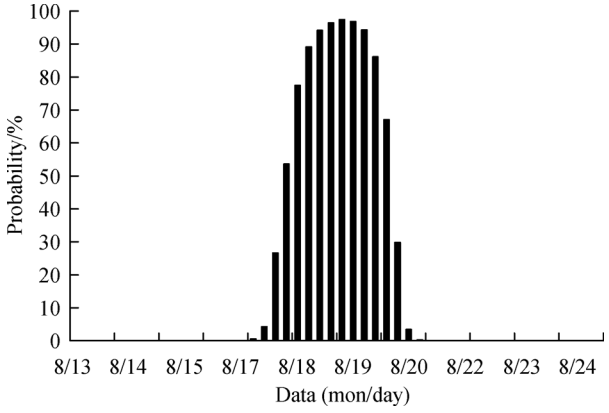

Fig. 9 Percentages above the warning threshold for the 2008 flood event.

discharges of rainfall-runoff models (Bartholmes et al., 2008; Thielen et al., 2008). The principle of equal probability of selection was applied in this study, in which the multiple inputs of the NFFS that had different structures were not taken into account. On the other hand, different weather forecasts are supposed to be assigned different weight coefficients, which might improve the performance of the grand ensemble in future studies. Flood forecasting demands a greater research effort in resolution and ensemble members to represent covariance of predictors and the extremes of distributions.

5 Conclusions

To meet the requirements for addressing uncertainty problems in flood forecasting based on single-model precipitation forecasting, a one-way coupled atmospheric-hydrological modeling system, based on combining high resolution with ensemble precipitation forecasting, is implemented in the hindcast analysis of the 2007 Huai River flood event.

Compared with the observed maximum 24-hour precipitation greater than 70 mm, the MC2 provided a good estimate in the fourth phase of July 5, with a relative percentage error of 9%. However, the precipitation amount was underestimated for the second phase and overestimated for the third phase of July 7. The GEM model underestimated precipitation amounts in the fourth phase of July 5 and the third phase of July 6. The T213 model shows its advantages in the second phase of July 7 and the first phase of July 8. The MC2 and the GEM and T213 model forecast success rates for the 24-hour accumulated precipitation amounts are 62.5%, 50%, and 56.25%, respectively. In most situations, the GEM and T213 models failed to perform better than the MC2 precipitation forecasts throughout the whole period, which could indicate that high-resolution models had better performances in evaluating the sensitivity in different initial conditions. Compared with the observed discharge, the MC2 forecast of July 5 had higher accuracy than the GEM and T213 models in peak discharge and timing. On July 6, the MC2 and the GEM and T213 models underestimated the observed peak discharge significantly, due to the severe precipitation underestimation on the third phase of July 6. The MC2 lagging peak discharge of July 7 could be attributed to the precipitation underestimation on the second phase and overestimation on the third phase. On the other hand, with prober discharge peak and timing forecasting, the GEM and T213 models filled the gap of instability of the MC2 on July 7.

The encouraging results obtained in this study demonstrate that combining high resolution with ensemble forecasts, based on the TIGGE database, provided a promising relative stability in flood forecasting. The coupled system was promising in the prediction of discharge peaks for warning purposes, while the ensemble hydrological forecasts provided a range of possible flood scenarios. Even though the signal was not persistent until four days before the peak discharge was observed in the 2007 flood event, the visualization based on threshold exceedance provided clear and concise essential warning information at an early stage, with 66% above the warning threshold and 28% above the alarm threshold. The signal was also able to represent the visualization of forecast persistence, which could be the real warning if it exceeds a certain percentage. The spread of different models was not scattered in the 2008 flood case, and the exact peak time fluctuated between August 18 and August 19, reaching to more than 50% probability. Most forecast members were closely clustered, with 62.5% of the members agreeing on the observed peak on August 15, 2008, which demonstrated a consistent intensive flood signal. As a result, the forecasters would be better prepared to predict the possibility of a flood at an early stage, and to subsequently issue a definitive warning if the signal strengthened, thus providing decision support for civil protection authorities.

Techniques need to be developed to address the combination of high resolution with ensemble forecasts. The principle of equal probability of selection was applied in this study, where multiple inputs of the NFFS having different structures were not taken into account. On the other hand, different weather forecasts should be assigned different weight coefficients, which may improve the performance of the GE in future studies. Flood forecasting demands a greater research effort in both resolution and the ensemble members to better represent covariance of predictors and the extremes of distributions.

Acknowledgements This work is supported by the Foundation for the Author of National Excellent Doctoral Dissertation of PR China (Grant No. 201161), the Program for New Century Excellent Talents in University (Grant No. NCET-12-0842), the Special Public Sector Research Program of Ministry of Water Resources (Grant Nos. 201301040, 201401008, and 201301070), the Natural Science Foundation of Jiangsu Province of China (Grant No. BK20131368), and the National Water Pollution Control and Management Technology Project of China (Grant No. 2012ZX07101-010).

References

Bao H J, Zhao L N, He Y, Li Z J, Wetterhall F, Cloke H L, Pappenberger F, Manful D (2011). Coupling ensemble weather predictions based on TIGGE database with Grid-Xinanjiang model for flood forecast. Adv Geosci, 29: 61–67

Bartholmes J, Thielen J, Ramos M, Gentilini S (2008). The European Flood Alert System EFAS – Part 2: statistical skill assessment of probabilistic and deterministic operational forecasts. Hydrol Earth Syst Sci Discuss, 5(1): 289–322

Benoit R, Desgagné M, Pellerin P, Pellerin S, Chartier Y, Desjardins S (1997). A semi-lagrangian, semi-implicit wide-band atmospheric model suited for fine scale process studies and simulation. Mon Weather Rev, 125(10): 2382–2415

Benoit R, Schär C, Binder P, Chamberland S, Davies H C, Desgagné M, Girard C, Keil C, Kouwen N, Lüthi D, Maric D, Müller E, Pellerin P, Schmidli J, Schubiger F, Schwierz C, Sprenger M, Walser A, Willemse S, Yu W, Zala E (2001). The real-time ultrafine scale forecast support during the special observing period of the MAP. Bull Am Meteorol Soc, 83(1): 985–1009

Bishop C H, Etherton B J, Majumdar S J (2001). Adaptive sampling with the ensemble transform Kalman filter Part I: theoretical aspects. Mon Weather Rev, 129(3): 420–436

Bourke W, Buizza R, Naughton M (2004). Performance of the ECMWF and the BoM ensemble prediction systems in the Southern Hemisphere. Mon Weather Rev, 132(10): 2338–2357

Branković Č, Palmer T N, Molteni F, Tibaldi S, Cubasch U (1990). Extended-range predictions with ECMWF models: time-lagged ensemble forecasting. Q J R Meteorol Soc, 116(494): 867–912

Buizza R, Palmer T N (1995). The singular-vector structure of the atmospheric global circulation. J Atmos Sci, 52(9): 1434–1456

Côté J, Gravel S, Méthot A, Patoine A, Roch M, Staniforth A (1998). The operational CMC-MRB Global Environmental Multiscale (GEM) model Part I: design considerations and formulation. Mon Weather Rev, 126(6): 1373–1395

Dalcher A, Kalnay E, Hoffman R N (1988). Medium range lagged forecasts. Mon Weather Rev, 116(2): 402–416

Davolio S, Miglietta M M, Diomede T, Marsigli C, Montani A (2012). A flood episode in Northern Italy: multi-model and single-model mesoscale meteorological ensembles for hydrological predictions. Hydrol Earth Syst Sci, 9(12): 13415–13450

Davolio S, Miglietta M M, Diomede T, Marsigli C, Morgillo A, Moscatello A (2008). A meteo-hydrological prediction system based on a multi-model approach for precipitation forecasting. Nat Hazards Earth Syst Sci, 8(1): 143–159

Diomede T, Davolio S, Marsigli C, Miglietta M M, Moscatello A, Papetti P, Paccagnella T, Buzzi A, Malguzzi P (2008b). Discharge prediction based on multi-model precipitation forecasts. Meteorol Atmos Phys, 101(3–4): 245–265

Diomede T, Marsigli C, Nerozzi F, Papetti P, Paccagnella T (2008a). Coupling high-resolution precipitation forecasts and discharge predictions to evaluate the impact of spatial uncertainty in numerical weather prediction model outputs. Meteorol Atmos Phys, 102(1–2): 37–62

Erfani A, Méthot A, Goodson R, Bélair S, Yeh K S, Côté J, Moffet R (2003). Synoptic and mesoscale study of a severe convective outbreak with the nonhydrostatic Global Environmental Multiscale (GEM) model. Meteorol Atmos Phys, 82(1–4): 31–53

Froude L (2010). TIGGE: comparison of the prediction of northern hemisphere extratropical cyclones by different ensemble prediction systems. Weather Forecast, 25(3): 819–836

Gill M A (1978). Flood routing by the Muskingum method. J Hydrol (Amst), 36(3–4): 353–363

Habets F, Noilhan J, Golaz C, Goutorbe J P, Lacarrère P, Leblois E, Ledoux E, Martin E, Ottlé C, Vidal-Madjar D (1999). The ISBA

surface scheme in a macroscale hydrological model applied to the Hapex-Mobilhy area Part 1: model and database. J Hydrol (Amst), 217(1–2): 75–96

He Y, Wetterhall F, Cloke H L, Pappenberger F, Wilson M, Freer J, McGregor G (2009). Tracking the uncertainty in flood alerts driven by grand ensemble weather predictions. Meteorol Appl, 16(1): 91–101

Krzysztofowicz R (2001). The case for probabilistic forecasting in hydrology. J Hydrol (Amst), 249(1–4): 2–9

Laprise R, Caya D, Bergeron G, Giguère M (1997). The formulation of the Andre Robert MC2 (Mesoscale Compressible Community) model. Atmos-ocean, 35(S1): 195–220

Li J, Zou Z L (2014). Impact of FY-3A MWTS radiances on prediction in GRAPES with comparison of two quality control schemes. Front Earth Sci, 8(2): 251–263

Liguori S, Rico-Ramirez M A (2013). A practical approach to the assessment of probabilistic flow predictions. Hydrol Processes, 27 (1): 18–32

Liu S Y, Gao W, Xu M, Wang X Y, Liang X Z (2009). China summer precipitation simulations using an optimal ensemble of cumulus schemes. Front Earth Sci, 3(2): 248–257

Liu Y, Duan Q, Zhao L, Ye A, Tao Y, Miao C, Mu X, Schaake J C (2013). Evaluating the predictive skill of post-processed NCEP GFS ensemble precipitation forecasts in China's Huai River Basin. Hydrol Processes, 27(1): 57–74

Luo B K, Qian X W (1987). Some problems with Muskingum method. Hydrological Sciences Journal, 32(4): 485–496

Ma S, Qu A, Wang Y (2007). The performance of the new tropical cyclone track prediction system of the China National Meteorological Center. Meteorol Atmos Phys, 97(1–4): 29–39

Ma Z K, Fan Z W, Zhang M, Su Y L (2014). Flood risk control of dams and dykes in middle reach of Huaihe River. Water Science and Engineering, 7(1): 17–31

Noilhan J, Planton S (1989). A simple parameterization of land surface processes for meteorological models. Mon Weather Rev, 117(3): 536–549

Pan X D, Li X, Shi X K, Han X J, Luo L H, Wang L X (2012). Dynamic downscaling of near-surface air temperature at the basin scale using WRF—A case study in the Heihe River Basin, China. Front Earth Sci, 6(3): 314–323

Pappenberger F, Bartholmes J, Thielen J, Cloke H L, Buizza R, de Roo A (2008). New dimensions in early flood warning across the globe using grand-ensemble weather predictions. Geophys Res Lett, 35 (10): L10404

Pappenberger F, Stephens E, Thielen J, Salamon P, Demeritt D, van Andel S J, Wetterhall F, Alfieri L (2013). Visualizing probabilistic flood forecast information: expert preferences and perceptions of best practice in uncertainty communication. Hydrol Processes, 27(1): 132–146

Pappenberger F, Thielen J, Del Medico M (2011). The impact of weather forecast improvements on large scale hydrology: analysing a decade of forecasts of the European Flood Alert System. Hydrol Processes, 25(7): 1091–1113

Park Y Y, Buizza R, Leutbecher M (2008). TIGGE: preliminary results on comparing and combining ensembles. Q J R Meteorol Soc, 134 (637): 2029–2050

Qaddouri A, Cote J, Valin M (2000). A parallel direct 3D elliptic solver. International Series in Engineering and Computer Science, 541: 429–442

Roebber P J, Schultz D M, Colle B A, Stensrud D J (2004). Toward improved prediction: high-resolution and ensemble modeling systems in operation. Weather Forecast, 19(5): 936–949

Rossa A, Liechti K, Zappa M, Bruen M, Germann U, Haase G, Keil C, Krahe P (2011). The COST 731 action: a review on uncertainty propagation in advanced hydro-meteorological forecast systems. Atmos Res, 100(2–3): 150–167

Si D, Ding Y H, Liu Y J (2009). Decadal northward shift of the Meiyu belt and the possible cause. Chin Sci Bull, 54(24): 4742–4748

Stensrud D J, Brooks H E, Du J, Tracton M S, Rogers E (1999). Using ensembles for short-range forecasting. Mon Weather Rev, 127(4): 433–446

Tanguay M, Robert A, Laprise R (1990). A semi-implicit semi-Lagrangian fully compressible regional forecast model. Mon Weather Rev, 118(10): 1970–1980

Thielen J, Bartholmes J, Ramos M, de Roo A (2008). The European flood alert system – part 1: concept and development. Hydrol Earth Syst Sci Discuss, 5(1): 257–287

Thomas S J, Girard C, Benoit R, Desgané M, Pellerin P (1998). A new adiabatic kernel for the MC2 model. Atmos-ocean, 36(3): 241–270

Todini E (2004). Role and treatment of uncertainty in real-time flood forecasting. Hydrol Processes, 18(14): 2743–2746

Wei M, Toth Z (2003). A new measure of ensemble performance: perturbation versus error correlation analysis (PECA). Mon Weather Rev, 131(8): 1549–1565

Wen L, Yu W, Lin C A, Béland M, Benoit R, Delage Y (2000). The role of land surface schemes in short-range, high spatial resolution forecast. Mon Weather Rev, 128(10): 3605–3617

Xuan Y, Cluckie D, Wang Y (2009). Uncertainty analysis of hydrological ensemble forecasts in a distributed model utilising short-range rainfall prediction. Hydrol Earth Syst Sci, 13(3): 293–303

Yakimiw E, Robert A (1986). Accuracy and stability analysis of a fully implicit scheme for the shallow-water equations. Mon Weather Rev, 114(1): 240–244

Yu Z B, Yang T, Schwartz F W (2014). Water issues and prospects for hydrological science in China. Water Science and Engineering, 7(1): 1–4

Zhang S L (2006). Interactive correct technology for flood forecasting. Shui Kexue Jinzhan, 17(5): 653–657 (in Chinese)

Zhang Y Y, Shao Q X, Xia J, Bunn S E, Zuo Q T (2011). Changes of flow regimes and precipitation in Huai River Basin in the last half century. Hydrol Processes, 25(2): 246–257

Zhao L N, Qi D, Tian F Y, Wu H, Di J Y, Wang Z, Li A H (2012). Probabilistic flood prediction in the upper Huaihe catchment using TIGGE data. Acta Meteorol Sin, 26(1): 62–71

Zhao R J (1992). The Xinanjiang model applied in China. J Hydrol (Amst), 135(1–4): 371–381